JAIST Repository
https://dspace.jaist.ac.jp/

Title	Explosive crystallization of amorphous silicon films by flash lamp annealing
Author(s)	Ohdaira, Keisuke; Fujiwara, Tomoko; Endo, Yohei; Nishizaki, Shogo; Matsumura, Hideki
Citation	Journal of Applied Physics, 106(4): 044907-1-044907-8
Issue Date	2009-08-25
Type	Journal Article
Text version	publisher
URL	http://hdl.handle.net/10119/8856
Rights	Copyright 2009 American Institute of Physics. This article may be downloaded for personal use only. Any other use requires prior permission of the author and the American Institute of Physics. The following article appeared in Keisuke Ohdaira, Tomoko Fujiwara, Yohei Endo, Shogo Nishizaki, and Hideki Matsumura, Journal of Applied Physics, 106(4), 044907 (2009) and may be found at http://link.aip.org/link/JAPIAU/v106/i4/p044907/s1
Description	

JAIST
JAPAN ADVANCED INSTITUTE OF SCIENCE AND TECHNOLOGY

Japan Advanced Institute of Science and Technology

Explosive crystallization of amorphous silicon films by flash lamp annealing

Keisuke Ohdaira,[a] Tomoko Fujiwara, Yohei Endo, Shogo Nishizaki, and Hideki Matsumura
Japan Advanced Institute of Science and Technology (JAIST), 1-1 Asahidai, Nomi, Ishikawa 923-1292, Japan

(Received 1 November 2008; accepted 10 July 2009; published online 25 August 2009)

Explosive crystallization (EC) takes place during flash lamp annealing in micrometer-thick amorphous Si (*a*-Si) films deposited on glass substrates. The EC starts from the edges of the *a*-Si films due to additional heating from flash lamp light. This is followed by lateral crystallization with a velocity on the order of m/s, leaving behind periodic microstructures in which regions containing several hundreds of nm-ordered grains and regions consisting of only 10-nm-sized fine grains alternatively appear. The formation of the dense grains can be understood as explosive solid-phase nucleation, whereas the several hundreds of nanometer-sized grains, stretched in the lateral direction, are probably formed through explosive liquid-phase epitaxy. This phenomenon will be applied to the high-throughput formation of thick poly-Si films for solar cells. © *2009 American Institute of Physics*. [DOI: 10.1063/1.3195089]

I. INTRODUCTION

The development of alternative energy resources to fossil fuel is one of the most important tasks to stop the global warming trend. Photovoltaic technology, directly yielding energy from sunlight, is the best candidate technology, and the production of solar cells has actually increased rapidly.[1] Many researchers have extensively studied the postcrystallization of precursor amorphous Si (*a*-Si) films deposited on glass substrates by high-throughput deposition techniques such as chemical vapor deposition (CVD) to form thin-film crystalline Si (*c*-Si) as a solar cell material.[2–4] Flash lamp annealing (FLA) is a promising technique for the high-throughput crystallization of precursor *a*-Si films, because of the suitable pulse duration on the order of milliseconds.[5–7] The thermal diffusion lengths L_T, defined as $L_T=(\kappa t/c\rho)^{1/2}$, where κ, t, c, and ρ represent thermal conductivity, duration, heat capacity, and density, respectively, of soda lime glass and *a*-Si in 5 ms are both on the order of several tens of μm. These values indicate that micrometer-order-thick *a*-Si films can be fully heated in millisecond annealing, whereas glass substrates, typically with a thickness of several millimeters, are not entirely heated. This feature is a great advantage compared with conventional rapid thermal annealing with duration on the order of seconds, which causes thermal damage to glass substrates, and compared with excimer laser annealing (ELA) with several tens of nanosecond duration, which results in insufficient heating of *a*-Si films in depth. We have actually realized crystallization of 4.5-μm-thick *a*-Si films by a single shot of flash lamp on quartz and soda lime glass substrates.[8,9] The polycrystalline Si (poly-Si) films indicate minority carrier lifetimes as long as 10 μs after defect termination through high-pressure water-vapor annealing.[10] We have also succeeded in fabricating prototype solar cells using the poly-Si films, demonstrating actual solar cell operation.[11]

Another interest in the rapid crystallization is a characteristic lateral crystallization, generally referred to as "explosive crystallization (EC)." This means lateral crystallization triggered by the heat corresponding to the enthalpy difference between two phases of material, released at the interface of the two phases. There have been a number of experimental reports concerning the EC using several types of pulse light sources such as *Q*-switched ruby lasers,[12–18] XeF excimer lasers,[19] frequency doubled or tripled Nd:YAG (yttrium aluminum garnet) lasers,[20–23] Nd-glass lasers,[24] and continuous-wave (cw) Ar ion lasers with scanning,[25–27] as well as many theoretical investigations.[28–32] Characteristic periodic surface structures with approximately 1 μm pitch spacing have been observed in the poly-Si films formed by FLA,[8,9,33] which may be an indication of the onset of the EC triggered by FLA because similar structures have been observed in the materials crystallized through EC.[18,23] In this study, we have investigated the surface appearances and the microstructures of the poly-Si films in order to clarify the crystallization mechanism of *a*-Si films by FLA. The experimental results clearly demonstrate the existence of centimeter-long lateral crystallization progressing from the Si film edges toward the center during FLA. The lateral movement of heat source is required for the centimeter-long lateral crystallization progressing within an annealing duration on the order of milliseconds, and we have to apply the concept of the EC for the explanation of that crystallization phenomenon. The poly-Si films are found to have periodic microstructures in which regions containing several hundreds of nm-ordered grains and regions consisting of only 10-nm-sized fine grains alternatively appear, indicating the existence of two EC modes.

II. EXPERIMENT

Quartz and soda lime glass substrates with a size of $20\times20\times0.7$ mm^3 were utilized as the substrates of the Si films. Since there is no significant dependence of the kind of

[a]Electronic mail: ohdaira@jaist.ac.jp.

 © 2009 American Institute of Physics

Downloaded 05 Apr 2010 to 150.65.7.70. Redistribution subject to AIP license or copyright; see http://jap.aip.org/jap/copyright.jsp

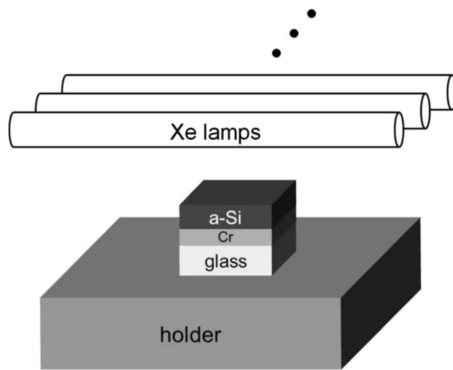

FIG. 1. Schematic of the FLA system used in this study. A Xe lamp array emits 5 ms pulse light having a broad spectrum in a visible range.

glass material on the crystallization results, poly-Si films formed on quartz substrates were mainly investigated in this study. Cr films with thicknesses of 60 or 200 nm were first deposited on the glass substrates by sputtering, aiming at the improvement of adhesion of Si films to glass substrates.[8,9] We have confirmed that the thickness of Cr does not greatly affect the crystallization results. Precursor *a*-Si films were then deposited on the Cr films by catalytic CVD (CAT-CVD), often called hot-wire CVD, which can produce *a*-Si films with low film stress and with a low hydrogen content of approximately 3%. These characteristics result in suppression of peeling of Si films during deposition and during FLA.[34] No dehydrogenation process was performed prior to FLA. The deposition rate of the *a*-Si films was approximately 100 nm/min. The other detailed deposition conditions are summarized elsewhere.[35]

FLA is a flash discharge from Xe lamps, emitting millisecond-order pulse having a broad spectrum in a visible range. The typical spectrum of the flash lamp light is seen elsewhere.[36] Figure 1 shows the schematic view of the FLA system used in this study. Samples are put on a holder, and receive pulse light emitted from a Xe lamp array in Ar atmosphere. The in-plane uniformity of the pulse light irradiance was fully satisfied in the sample area of $20 \times 20\ \text{mm}^2$. *a*-Si films formed on Cr-coated glass substrates absorb the pulse light, which results in rapid increase in the film temperature. Figure 2 shows the absorption spectrum of a 4.5-μm-thick *a*-Si film that was formed directly on a quartz substrate. FLA was performed with a fixed pulse duration of 5 ms, whereas

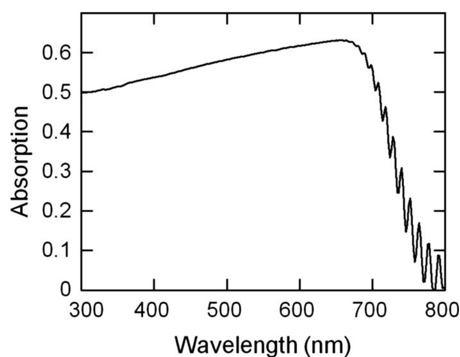

FIG. 2. Absorption spectrum of an *a*-Si film formed directly on a quartz substrate.

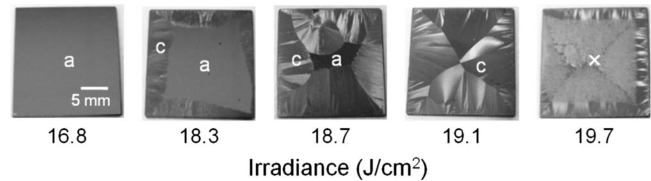

FIG. 3. Surface images of the Si films after FLA under various flash lamp irradiances. "a", "c", and "x" represent amorphous, crystallized, and peeled parts, respectively.

its irradiance was systematically changed around $19\ \text{J/cm}^2$. Only one shot of flash lamp was supplied for each sample. Unfortunately, the actual temperature of the Si films during FLA could not be measured due to lack of an *in situ* measurement system. The microstructures of the crystallized films were characterized by atomic force microscopy (AFM) and transmission electron microscopy (TEM). The crystallization and crystallinity of the Si films were characterized by Raman spectroscopy using a He–Ne laser with a beam spot size of about 1 μm.

III. RESULTS

Figure 3 shows the surface images of the Si films after FLA under various lamp irradiances. Only the edges are crystallized in the case of the lowest lamp irradiance, and the crystallized area expands toward the center of the Si films with increase in lamp irradiance. This fact clearly shows that the crystallization of the *a*-Si films by FLA takes place laterally from the edges toward the center. The process window for the observation of the lateral crystallization is very narrow, within $\pm 0.5\ \text{J/cm}^2$, because Si films peel off during FLA under higher irradiance. Thus, unfortunately, we cannot currently discuss the actual process window for the onset of the lateral crystallization, and further improvement in the adhesion of Si films is required for the detailed discussion of the process window.

Figure 4 shows a cross-sectional TEM image of the poly-Si film formed by FLA, indicating that the poly-Si film consists of small grains with sizes less than 1 μm. The grainlike structures shown in the surface images of Fig. 3 are therefore not grains, but characteristic patterns formed through the lateral crystallization. The projecting parts can be seen on the surface of the poly-Si film, together with highly dense voids located just below the projections. The projections are formed quite periodically with a pitch of approximately 1 μm. These act as optical gratings, and thus, form typical grainlike surface appearances. This typical surface structure is also observed in the AFM image of the poly-Si film as shown in Fig. 5. There is no significant change in the spacing of the surface periodic structures within the process window. The second characteristic microstructure of the poly-Si films is the existence of two kinds of regions; one contains relatively large grains, with a size on the order of several hundreds of nm, represented as black and light gray contrasts in the TEM image (region *L*), and the other consists only of 10-nm-sized fine grains with uniform dark gray color (region *F*). Region *L* connects to the surface projecting regions, while region *F* areas lie below the flat

Downloaded 05 Apr 2010 to 150.65.7.70. Redistribution subject to AIP license or copyright; see http://jap.aip.org/jap/copyright.jsp

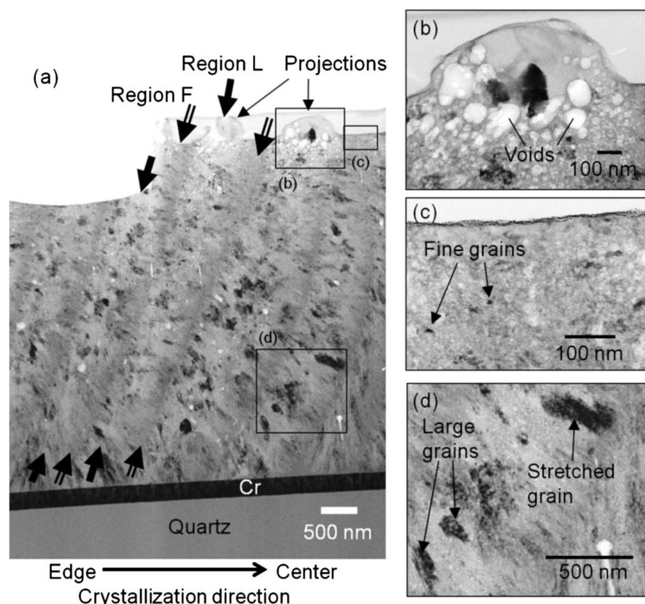

FIG. 4. Cross-sectional TEM image of the poly-Si film formed by FLA. There exist 1-μm-pitch projections on the surface. One can also observe region *L* (containing large stretched grains) and region *F* (consisting of 100 nm sized fine grains), which are indicated using single- and double-line arrows, respectively.

region. The relatively large grains tend to be stretched in the lateral crystallization direction, which is also a clear indication of lateral crystallization. The third characteristic fact about the microstructure is that the two typical characteristic regions have curvatures toward the edge direction.

Figure 6 shows Raman spectra of the poly-Si film formed by FLA under the lowest irradiance in Fig. 3, measured at points close to an *a*-Si/*c*-Si boundary, together with the corresponding surface macro- and microscopic images indicating the measurement positions. The surface periodic roughness can be clearly seen in the microscopic image of the poly-Si region. The Raman spectra show high crystallinity close to unity in the poly-Si region, and show no gradual decrease in the crystallinity even close to the *a*-Si/*c*-Si interface, whereas there are no *c*-Si peaks in the Raman spectra measured in the *a*-Si region, indicating significantly abrupt change in the phases from *a*-Si to *c*-Si at the boundary.

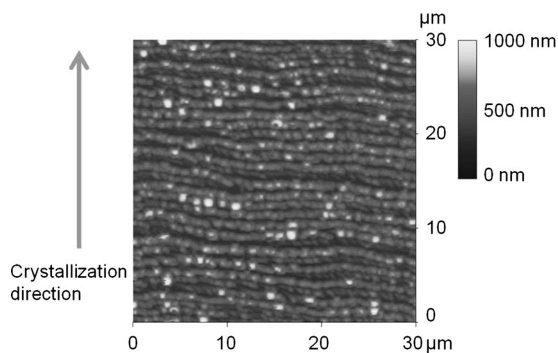

FIG. 5. AFM image of the poly-Si surface, indicating 1-μm-spaced periodic microstructures along the crystallization direction.

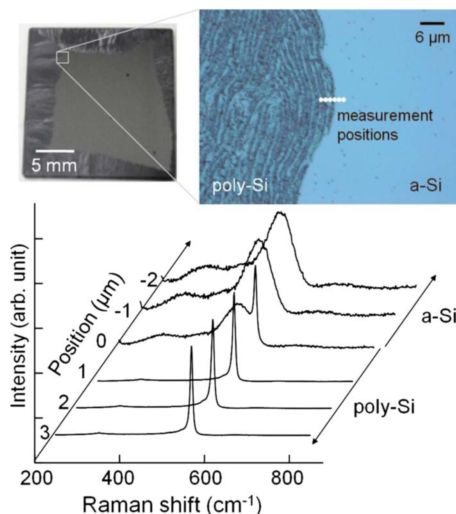

FIG. 6. (Color online) Raman spectra measured in the vicinity of the *a*-Si/*c*-Si interface. The corresponding macroscopic and microscopic images are also shown.

IV. DISCUSSION

A. Elimination of the possibility of simple melting growth and of solid-phase crystallization

One of the most popular crystallization mechanisms is the solidification from molten Si, typically taking place in the case of ELA of thin (<100 nm) *a*-Si films. In our case, however, crystallization after complete melting of the whole Si is unlikely, since the dopant profiles for boron (B) and phosphorus (P) show no significant change after FLA, as has already been reported.[11] The diffusion coefficients of B and P in Si melt are 2.4×10^{-4} and 5.1×10^{-4} cm^2/s,[37] corresponding to the diffusion lengths of 11 and 16 μm in 5 ms, respectively. The profiles of the dopants will therefore be completely broken if the whole Si film is melted during the annealing time of 5 ms.

Another frequently discussed crystallization mechanism is solid-phase crystallization (SPC), meaning jumping of Si atoms from *a*-Si into *c*-Si phases via defects. The SPC, however, cannot describe the formation of the projecting surface structures, since such drastic change in surface morphology is probably induced via melting of Si. The lateral crystallization also cannot be explained by these simple crystallization mechanisms, and we have to consider other profound crystallization processes.

B. Crystallization starting from the edges

Before considering the mechanism of the lateral expansion of the crystallized areas, we should clarify why the crystallization starts mainly from the edges of the Si films. The temperature of *a*-Si has to reach a threshold value to start crystallization, such as the melting point of *a*-Si in the case of melting growth, or the temperature required for a sufficient nucleation rate in the case of SPC. Thus, the experimental results indicate that the edges of Si have higher temperature than the interior areas, which is well explained by the additional heating of the Si film edges by the lamp irradiation. Figure 7(a) schematically shows the irradiation of

Downloaded 05 Apr 2010 to 150.65.7.70. Redistribution subject to AIP license or copyright; see http://jap.aip.org/jap/copyright.jsp

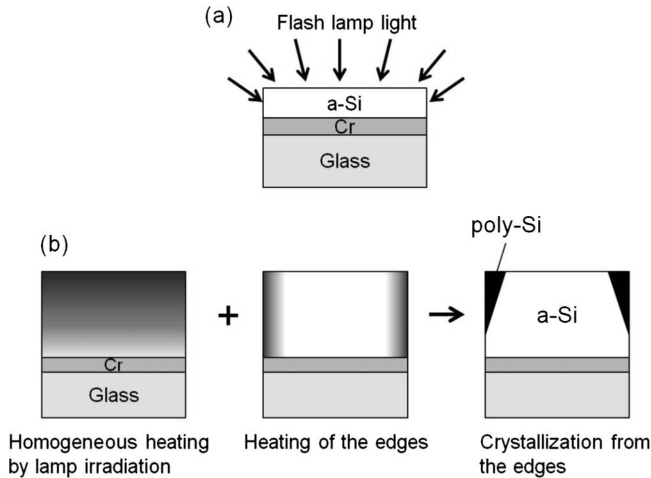

FIG. 7. (a) Schematic image of the flash lamp irradiation to an *a*-Si film, indicating that angled irradiation heats the edges. (b) Schematics of the heat generation due to irradiation at the surface and at the edges, and of the crystallization starting at the edges.

flash lamp light onto the *a*-Si films on glass substrates. The *a*-Si film is heated by the absorption of the irradiated light with high homogeneity in the lateral direction, and has an in-depth distribution of temperature determined by the duration of irradiation and the thermal diffusivities of *a*-Si, Cr, and glass. Although the L_T of *a*-Si during millisecond-order annealing is on the order of several tens of microns, we also have to consider the effect of the inserted Cr films with great thermal conductivity. We have actually confirmed lower crystallinity of the bottom regions of the Si films, especially in the vicinity of the Si/Cr interface, than of the top regions,[38] indicating insufficient in-depth uniformity of the temperature of the Si films. The distribution of the temperature is schematically drawn at the left of Fig. 7(b). The edges of the Si films also receive additional heating, as shown in Fig. 7(a), because flash lamp light expands from the lamp arrays, and the angle of incidence must be considered. The thermal distribution due to the heating of the edges is schematically drawn in the center of Fig. 7(b). Combining these two heating processes, the top corner must have the highest temperature, probably resulting in triangle-shaped areas, as schematically shown at the right of Fig. 7(b). The curvature observed in the microstructure probably reflects the initial shape of the crystallized areas.

To check whether the edges actually undergo thermal gains, we also have to consider thermal losses due to convection and radiation from the edges, which can be represented in the following equations:

$$q_{\mathrm{conv}} = hA(T - T_\infty), \quad (1)$$

$$q_{\mathrm{rad}} = \sigma A(T^4 - T_\infty^4), \quad (2)$$

where h represents a heat transfer coefficient, which can be approximated to be $h = 1.32\{(T - T_\infty)/L\}^{1/4}$ using a sample length L,[39] A the area, σ the Stefan–Boltzmann constant, T the temperature of Si, and T_∞ the temperature of ambient atmosphere, respectively. Even if taking the values of T and T_∞ to be the melting point of *c*-Si (1687 K) and room temperature (300 K), the losses due to convection and radiation are estimated to be 1.66 and 45.9 W/cm^2, corresponding to the energy losses of 1.49×10^{-2} and 0.229 J/cm^2 in 5 ms, respectively. These values are negligibly small compared to the energy of flash lamp irradiation, on the order of several tens of J/cm^2, indicating that heat generation is probably dominant on the edges, and that the proposed model for describing the starting of the crystallization is reasonable.

C. Possible mechanism of the lateral crystallization

Next, we discuss the mechanism of the lateral expansion of the crystallized regions. The simplest model is thermal diffusion from the edge to the interior area of the Si films, since the film edges are continuously heated during the 5 ms duration. Thus, we consider the L_T of the relevant materials in 5 ms in order to check whether the middle part of the *a*-Si region 1 cm from the edges can receive the heat generated at the edges during 5 ms. The L_T are summarized in Table I,[7,40,41] all the values of which cannot explain centimeter-order lateral crystallization. This estimation also indicates that the movement of the heat source during 5 ms is necessary to explain the lateral crystallization over such a long distance.

The only mechanism for describing the heat generation other than absorption of lamp irradiation is heating due to differences of enthalpy between the *a*-Si and *c*-Si states. *a*-Si is a metastable state, and hence has higher enthalpy than *c*-Si, resulting in thermal generation due to crystallization. The generated heat diffuses into the neighboring area, and

TABLE I. Thermal diffusion lengths of the relevant materials in 5 ms and in 0.5 μs. The characteristic values of the materials for the calculation of the diffusion length are also summarized. The values for *a*-Si, *c*-Si, and Cr are at 1000 °C, and those for SiO_2 are at room temperature.

Material	L_T in 5 ms (μm)	L_T in 0.5 μs (μm)	Thermal conductivity (W/cm K)	Density (g/cm^3)	Heat capacity (J/g K)
a-Si [a]	47	0.47	0.011	2.30	1.07
c-Si [a]	240	2.4	0.25	2.30	0.96
Liquid Si[a]	340	3.4	0.56	2.56	0.92
Cr[b]	240	⋯	0.60	7.19	0.71
SiO_2 [a]	66	⋯	0.014	2.20	0.74

[a]Reference 7.
[b]References 40 and 41.

Downloaded 05 Apr 2010 to 150.65.7.70. Redistribution subject to AIP license or copyright; see http://jap.aip.org/jap/copyright.jsp

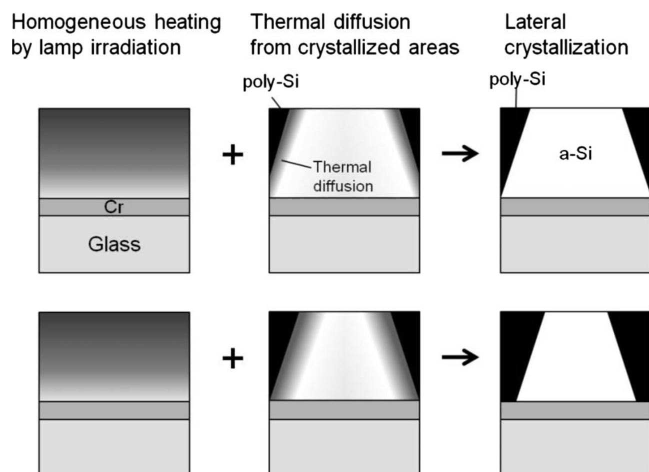

FIG. 8. Schematics of the supposed mechanism of lateral crystallization. Heat generation due to crystallization induces further crystallization of neighboring *a*-Si.

induces further crystallization. The possible dominolike crystallization mechanism is schematically represented in Fig. 8. 1 cycle of heat generation and its diffusion probably corresponds to the characteristic periodic structure shown in Fig. 4. The 1-cm-long lateral crystallization therefore corresponds to 10 000 cycles of the formation of a set of the 1-μm-pitch poly-Si structure, and thus, that 1 cycle must be performed within 0.5 μs. To check the validity of the proposed mechanism, we also summarized the L_T of Si in 0.5 μs under various Si phases in Table I. The estimated values are quite close to the 1 cycle pitch length of 1 μm. Although the L_T of *a*-Si is slightly smaller than 1 μm, the actual L_T must be affected both by the nature of *c*-Si and by that of *a*-Si. Hence, the proposed model can fully describe the cm-order lateral crystallization during 5 ms. One may question whether the crystallization really takes place within the millisecond-order duration. To answer it, we should consider the character of nonthermal equilibrium treatment. According to Table I, the thermal diffusion length of quartz in 5 ms is only 66 μm, which means that the most part of the 700-μm-thick quartz substrate keeps the temperature sufficiently low, close to room temperature, even immediately after finishing the pulse irradiation. Due to the absence of heat source for the Si film and the large difference of temperature between the Si film and the quartz substrates, the temperature of the Si film decreases quite rapidly by thermal diffusion to the substrate. For instance, thermal diffusion length of quartz in 20 ms is estimated to be 132 μm, twice the value in 5 ms. This indicates that the temperature of Si becomes roughly half, which is sufficient to stop the nucleation and crystallization of *a*-Si. We can therefore safely conclude that the crystallization is completed within millisecond-order duration.

Shock waves triggered by a high-power pulse laser irradiation can also induce quite rapid lateral crystallization, which also leaves behind periodic structures perpendicular to the lateral crystallization direction.[42] However, this is the phenomenon in the case of much higher laser peak power, on the order of 1×10^{13} W/cm^2 (1 kJ/cm^2, 100 ps), rather than that of FLA of less than 1×10^4 W/cm^2. The effect of shock waves therefore seems to be unlikely in the case of FLA.

D. Explosive crystallization

As we have mentioned in the Introduction, the lateral crystallization based on heat generation due to crystallization has been well known as EC. The observed lateral crystallization velocity, on the order of m/s, can be fully explained as EC.[12–32] Geiler *et al.*[24] proposed the following four types of EC: (1) explosive solid-phase nucleation (ESPN), governed by nucleation directly from *a*-Si to *c*-Si phase; (2) explosive solid-phase epitaxy, in which epitaxial growth in solid phase is dominant; (3) explosive liquid-phase nucleation (ELPN), dominated by nucleation from Si melt; and (4) explosive liquid-phase epitaxy (ELPE), in which liquid-phase epitaxy governs the crystallization. As has been already mentioned, the poly-Si films contain two characteristic regions (regions *L* and *F*), which probably means that at least two different types of EC are alternately taking place during FLA. Region *F* is obviously governed by nucleation, and thus, formed through ESPN or ELPN. Region *L* is probably formed through partial or complete melting of *a*-Si, because of the significant change in the surface morphology. The large-sized grains extending in the lateral crystallization directions can be explained only by epitaxial growth.

To discuss the reasons for the existence of two different types of poly-Si regions, we will consider degree of heat generation through the EC modes. Considering the abrupt phase change at the *a*-Si/*c*-Si boundary shown in Fig. 6, the temperature of Si before receiving the lateral heat transfer must be less than the melting point of *a*-Si. Based on the proposed crystallization mechanism and on the cross-sectional TEM image shown in Fig. 4, the emitted heat from the microstructure 1 μm in width induces the next 1-μm-width crystallization. The emitted heat due to crystallization is estimated to be 6–10 kJ/mol assuming SPC, or 0–6 kJ/mol in the case of crystallization from supercooled Si melt.[24,43] These estimates are much smaller than the latent heat of fusion of *a*-Si (35.4 kJ/mol).[24] This fact indicates that the heat generated due to crystallization is not strong enough to completely melt the neighboring *a*-Si of the same width, and hence, the crystallization takes place from mixed phases of *a*-Si and supercooled Si melt, or only from *a*-Si through SPC. Region *F* is therefore formed through ESPN, while region *L* formed is through simultaneous ESPN and ELPE. Of course, we should consider the possibility of the melting crystallization of Si film edges triggered by the additional flash lamp irradiation, which might result in the melting of the neighboring *a*-Si. However, the heat at the edges is never conducted to *a*-Si at a few millimeters away from the edges within the millisecond-order duration, because of the insufficient thermal diffusion lengths of *a*-Si and Si melt of less than 1 mm, as shown in Table I, and thus, the *a*-Si can receive only the heat generated due to crystallization from neighboring *c*-Si. Furthermore, we have confirmed same periodic patterns very close to the Si film edges. This fact probably indicates that the crystallization is governed by the same mechanism throughout the whole crystallization process. The

Downloaded 05 Apr 2010 to 150.65.7.70. Redistribution subject to AIP license or copyright; see http://jap.aip.org/jap/copyright.jsp

surface projections are probably formed through volume expansion from Si melt to *c*-Si, leaving voids just below the projections. Auvert *et al.*[27] also observed the mixed feature of liquid-phase and solid-phase ECs in cw laser crystallization, and found that the poly-Si formed through liquid-phase crystallization has a rough surface, whereas the SPC region shows a smooth surface, supporting our explanation. The B and P diffusions during 0.5 μs are estimated to be 0.11 and 0.16 μm, respectively, even if Si is completely melted during the 0.5 μs. The unchanged dopant profiles, shown in Ref. 11, are therefore consistent with the proposed crystallization model.

To numerically check the validity of the proposed crystallization mechanism, the solid-phase nucleation rate is estimated using the classical nucleation theory.[44] Grain size distribution, that is, grain density per unit grain radius as a function of grain radius, is expressed as[44]

$$n(R,t) = \frac{N_a O_{i^*}\left(\frac{\Delta g_v}{6\pi kTi^*}\right)^{1/2} \exp\left(-\frac{\Delta G^*}{kT}\right)\exp\left[-\exp\left(-\frac{t-t_{\mathrm{inc}}(R)}{\tau_S}\right)\right]}{\frac{a\Delta g_v}{kT}\left(1-\frac{R^*}{R}\right)}, \tag{3}$$

where T is temperature, N_a is the Si atomic density, i^* is the number of atoms in a critical cluster size, O_i^* is the number of surface atoms in a cluster containing i^* atoms, Δg_v is the free energy change associated with the crystallization of one atom, a is the average atomic distance (0.27 nm), R is the grain radius, R^* is the grain radius at a critical cluster size i^*, and $\Delta G^* = 16\pi\sigma_{ca}{}^3/3\Delta g_v{}^2$ is the free energy of a cluster containing i^* atoms, σ_{ca} being the interface free energy of each atom at the *c*-*a* interface. t_{inc} and τ_S represent the incubation time and the transient time, both of which are related to Δg_v, σ_{ca}, Λ, f, and T, where Λ is the volume transformed by each defect jump to the *c*-Si or to the *a*-Si phase, and $f = f_0 \exp(-E_m/kT)$ is the thermally activated defect jump frequency, E_m being the activation energy. The crystalline fraction of the Si film (X_c) can be written as

$$X_c(t) = \int_0^\infty \frac{4}{3}\pi R^3 n(R,t)dR, \tag{4}$$

if neglecting the depletion of *a*-Si. For the above calculation, we used the parameters summarized in Table II.[44–46] T is taken to be the melting point of *a*-Si, that is, the maximum temperature for SPC. This assumption is reasonable since region L is partially, but not completely melted according to the discussed model, and region F neighbors region L.

Figure 9 shows the X_c for various C_{av}, calculated using Eq. (4). The calculation result indicates that C_{av} on the order of $10^{20}/\mathrm{cm}^3$ or more is necessary for the SPC during 0.5 μs, which is the duration required for 1 cycle of the lateral crystallization. Because the thermal diffusion process also has to be performed within the 0.5 μs, the actual required value for the C_{av} must be close to $10^{21}/\mathrm{cm}^3$. This value is much higher than the defect density initially contained in the precursor *a*-Si films of $1\times10^{16}/\mathrm{cm}^3$ or less. This fact indicates that structural defects are newly generated during FLA. Recently, we have confirmed the actual decrease in the number of Si–H bonds on the order of $10^{21}/\mathrm{cm}^3$ in the Si films after FLA,[47] which fully explain the C_{av}. Figure 9 also indicates necessity of sufficient duration, approximately 0.055 μs in this case, to realize a sufficient X_c close to unity. This fact might be a description of the intermittent lateral movement of the *c*-Si/*a*-Si interface, that is, heat generation is delayed by the duration needed for crystallization after the heat transfer into the neighboring *a*-Si regions. Figure 10 shows the grain size distribution in the poly-Si film calculated using Eq. (3) for $C_{\mathrm{av}} = 10^{21}/\mathrm{cm}^3$ and $t = 0.055$ μs. The results indicate that the radius of the grains formed in this duration is limited to be less than 20 nm. Region F is therefore quantitatively reasonable to consider its formation mechanism as ESPN, while

TABLE II. Parameters for the calculation of X_c and grain size distribution.

Parameters	Values	Ref.
Δg_v	0.0985 eV	44–46
σ_{ca}	0.1075 eV	44–46
Λ	6×10^{-23} cm^3	44
E_m	1.36 eV	44
f_0	$2\times10^{15}/\mathrm{s}$	44
T	1418 K	⋯

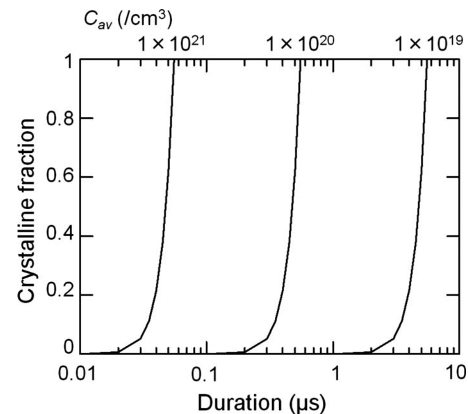

FIG. 9. X_c as a function of annealing duration for various C_{av}, calculated based on the classical nucleation theory.

Downloaded 05 Apr 2010 to 150.65.7.70. Redistribution subject to AIP license or copyright; see http://jap.aip.org/jap/copyright.jsp

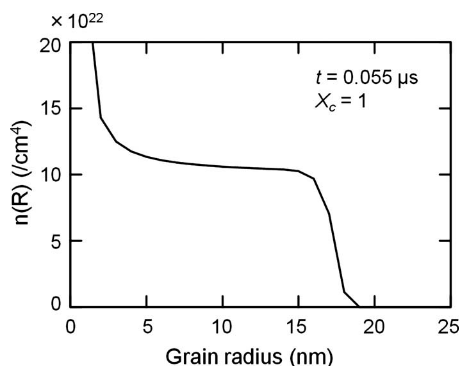

FIG. 10. Calculated grain size distribution in a poly-Si, for $C_{av}=10^{21}/\mathrm{cm}^3$ and $t=0.055$ μs.

region L, which contains grains with sizes more than 100 nm, is found to be governed by a mechanism other than the ESPN, including liquid-phase process. These facts are completely consistent with the discussed crystallization mechanism.

We will finally discuss the enlargement of the crystallization area for formation of large-area poly-Si films to be applied in solar cells. Based on our understanding of the crystallization mechanism discussed above, the lateral crystallization continues until the temperature of a-Si reaches a threshold temperature, probably the melting point of a-Si, after receiving the lateral heat transfer. This means that the key factor for the enlargement of the crystallized area is to keep the temperature of a-Si sufficiently high as long as possible. Preheating of the samples and increase in the pulse duration will therefore result in the enlargement of the crystallized area. Another approach is formation of starting points for lateral crystallization at locations other than the a-Si film edges by supplying local heating using additional pulse lasers, for instance, at the same time as the FLA. If we can start the lateral crystallization from the intended areas, further large-area crystallization will be realized.

V. CONCLUSION

We have observed rapid lateral crystallization, on the order of m/s, of μm-thick a-Si films formed on glass substrates by FLA. The crystallization starts from the edges of the Si films, probably due to receiving additional flash lamp light. The lateral crystallization cannot be caused by lateral thermal diffusion from the edges, and therefore, heat generation due to crystallization and its transfer into neighboring a-Si; that is, EC, governs the crystallization. Periodic microstructures with approximately 1 μm pitch are formed through the EC. The nucleation process probably occurs through ESPN, whereas relatively large grains, stretched in the lateral crystallization direction, are formed through simultaneous ESPN and ELPE. Based on the crystallization mechanism proposed, enlargement of the crystallization area will be possible by keeping the temperature of a-Si high enough as long as possible, and by forming additional starting points of the crystallization intentionally.

ACKNOWLEDGMENTS

The authors acknowledge T. Owada and T. Yokomori of Ushio Inc. for their expert operation of and helpful discussion on FLA, and Professor M. A. Mooradian for improvement of English. This work was in part supported by the New Energy and Industrial Technology Development Organization (NEDO) of Japan.

[1]W. Hoffmann, Sol. Energy Mater. Sol. Cells **90**, 3285 (2006).
[2]L. Carnel, I. Gordon, D. Van Gestel, G. Beaucarne, and J. Poortmans, Proceedings of the 22nd European Photovoltaic Solar Energy Conference, 2007, p. 1880.
[3]I. Gordon, D. Van Gestel, L. Carnel, G. Beaucarne, J. Poortmans, K. Y. Lee, P. Dogan, B. Gorka, C. Becker, F. Fenske, B. Rau, S. Gall, B. Rech, J. Plentz, F. Falk, and D. Le Bella, Proceedings of the 22nd European Photovoltaic Solar Energy Conference Exhibition, 2007, p. 1890.
[4]M. J. Keevers, T. L. Young, U. Schubert, and M. A. Green, Proceedings of the 22nd European Photovoltaic Solar Energy Conference Exhibition, 2007, p. 1783.
[5]F. Terai, S. Matsunaka, A. Tauchi, C. Ichikawa, T. Nagatomo, and T. Homma, J. Electrochem. Soc. **153**, H147 (2006).
[6]B. Pécz, L. Dobos, D. Panknin, W. Skorupa, C. Lioutas, and N. Vouroutzis, Appl. Surf. Sci. **242**, 185 (2005).
[7]M. Smith, R. McMahon, M. Voelskow, D. Panknin, and W. Skorupa, J. Cryst. Growth **285**, 249 (2005).
[8]K. Ohdaira, Y. Endo, T. Fujiwara, S. Nishizaki, and H. Matsumura, Jpn. J. Appl. Phys., Part 1 **46**, 7603 (2007).
[9]K. Ohdaira, T. Fujiwara, Y. Endo, S. Nishizaki, and H. Matsumura, Jpn. J. Appl. Phys. **47**, 8239 (2008).
[10]Y. Endo, T. Fujiwara, S. Nishizaki, K. Ohdaira, K. Nishioka, and H. Matsumura, Technical Digest of 17th International Photovoltaic Science and Engineering Conference, 2007, p. 319.
[11]K. Ohdaira, T. Fujiwara, Y. Endo, K. Shiba, H. Takemoto, S. Nishizaki, Y. R. Jang, K. Nishioka, and H. Matsumura, Proceedings of the 33rd IEEE Photovoltaic Specialists Conference, 2008, p. 418.
[12]A. Aydinli, M. Berti, A. V. Drigo, R. Lotti, and P. G. Merli, J. Appl. Phys. **64**, 3301 (1988).
[13]P. A. Stolk, A. Polman, W. C. Sinke, C. W. T. Bulle-Lieuwma, and D. E. W. Vandenhoudt, Mater. Res. Soc. Symp. Proc. **147**, 179 (1989).
[14]A. Polman, D. J. W. Mous, P. A. Stolk, W. C. Sinke, C. W. T. Bulle-Lieuwma, and D. E. W. Vandenhoudt, Appl. Phys. Lett. **55**, 1097 (1989).
[15]K. Murakami, O. Eryu, K. Takita, and K. Masuda, Phys. Rev. Lett. **59**, 2203 (1987).
[16]J. J. P. Bruines, R. P. M. van Hai, H. M. J. Boots, A. Polman, and F. W. Saris, Appl. Phys. Lett. **49**, 1160 (1986).
[17]M. O. Thompson, G. J. Galvin, J. W. Mayer, P. S. Peercy, J. M. Poate, D. C. Jacobson, A. G. Cullis, and N. G. Chew, Phys. Rev. Lett. **52**, 2360 (1984).
[18]T. Takamori, R. Messier, and R. Roy, Appl. Phys. Lett. **20**, 201 (1972).
[19]C. C. Kuo, W. C. Yeh, J. B. Chen, and J. Y. Jeng, Thin Solid Films **515**, 1651 (2006).
[20]W. Marine and J. Marfaing, Mater. Res. Soc. Symp. Proc. **157**, 449 (1990).
[21]J. J. P. Bruines, R. P. M. Van Hal, B. H. Koek, M. P. A. Viegers, and H. M. J. Boots, Mater. Res. Soc. Symp. Proc. **74**, 91 (1987).
[22]J. J. P. Bruines, R. P. M. van Hai, B. H. Koek, M. P. A. Viegers, and H. M. J. Boots, Appl. Phys. Lett. **50**, 507 (1987).
[23]C. Grigoropoulos, M. Rogers, S. H. Ko, A. A. Golovin, and B. J. Matkowsky, Phys. Rev. B **73**, 184125 (2006).
[24]H.-D. Geiler, E. Glaser, G. Götz, and W. Wagner, J. Appl. Phys. **59**, 3091 (1986).
[25]D. Bensahel, G. Auvert, A. Perio, J. C. Pfister, A. Izrael, and P. Henoc, J. Appl. Phys. **54**, 3485 (1983).
[26]D. Bensahel, G. Auvert, and M. Dupuy, J. Appl. Phys. **54**, 395 (1983).
[27]G. Auvert, D. Bensahel, A. Perio, V. T. Nguyen, and G. A. Rozgonyi, Appl. Phys. Lett. **39**, 724 (1981).
[28]E. J. Albenze, M. O. Thompson, and P. Clancy, Ind. Eng. Chem. Res. **45**, 5628 (2006).
[29]E. J. Albenze, M. O. Thompson, and P. Clancy, Phys. Rev. B **70**, 094110 (2004).
[30]J. Y. Tsao and P. S. Peercy, Phys. Rev. Lett. **58**, 2782 (1987).
[31]K. H. Heinig and H.-D. Geiler, Phys. Status Solidi A **92**, 421 (1985).
[32]K. H. Heinig and H.-D. Geiler, Phys. Status Solidi A **93**, 99 (1986).

Downloaded 05 Apr 2010 to 150.65.7.70. Redistribution subject to AIP license or copyright; see http://jap.aip.org/jap/copyright.jsp

[33]K. Ohdaira, T. Fujiwara, Y. Endo, S. Nishizaki, K. Nishioka, and H. Matsumura, Technical Digest of 17th International Photovoltaic Science and Engineering Conference, 2007, p. 1326.
[34]K. Ohdaira, K. Shiba, H. Takemoto, T. Fujiwara, Y. Endo, S. Nishizaki, Y. R. Jang, and H. Matsumura, Thin Solid Films **517**, 3472 (2009).
[35]K. Ohdaira, S. Nishizaki, Y. Endo, T. Fujiwara, N. Usami, K. Nakajima, and H. Matsumura, Jpn. J. Appl. Phys., Part 1 **46**, 7198 (2007).
[36]H. Habuka, A. Hara, T. Karasawa, and M. Yoshioka, Jpn. J. Appl. Phys., Part 1 **46**, 937 (2007).
[37]H. Kodera, Jpn. J. Appl. Phys. **2**, 212 (1963).
[38]T. Fujiwara, Y. Endo, S. Nishizaki, K. Ohdaira, K. Nishioka, and H. Matsumura, Technical Digest of 17th International Photovoltaic Science and Engineering Conference, 2007, p. 1157.
[39]J. P. Holman, *Heat Transfer*, 8th ed. (McGraw-Hill, New York, 1997).
[40]O. Madelung and G. K. White, *Thermal Conductivity of Pure Metals and Alloys*, Landolt-Börnstein, New Series, Group III, Vol. 15c (Springer-Verlag, Berlin, 1991).
[41]I. S. Grigoriev and E. Z. Meilikhov, *Handbook of Physical Quantities* (CRC, Boca Raton, FL, 1997).
[42]Y. Kanemitsu, Y. Tanaka, and H. Kuroda, Jpn. J. Appl. Phys., Part 2 **24**, L959 (1985).
[43]E. P. Donovan, F. Spaepen, D. Turnbull, J. M. Poate, and D. C. Jacobson, Appl. Phys. Lett. **42**, 698 (1983).
[44]C. Spinella and S. Lombardo, J. Appl. Phys. **84**, 5383 (1998), and references therein.
[45]E. P. Donovan, F. Spaepen, D. Turnbull, J. M. Poate, and D. C. Jacobson, J. Appl. Phys. **57**, 1795 (1985).
[46]E. P. Donovan, F. Spaepen, J. M. Pate, and D. C. Jacobson, Appl. Phys. Lett. **55**, 1516 (1989).
[47]K. Ohdaira, H. Takemoto, K. Shiba, and H. Matsumura, Appl. Phys. Express **2**, 061201 (2009).

Downloaded 05 Apr 2010 to 150.65.7.70. Redistribution subject to AIP license or copyright; see http://jap.aip.org/jap/copyright.jsp